Hindawi
International Journal of Chemical Engineering
Volume 2022, Article ID 9812188, 9 pages
https://doi.org/10.1155/2022/9812188

Research Article

Interaction Study of Oxygen and Iron-Sulfur Clusters Based on the Density Functional Theory

Jiancun Gao,[1,2] **Hongbin Sui**,[1] **Siyuan Wu**,[1,2] **Renyou Zhang**,[1,2] **Mengxin Zhang**,[1] **Bolun Cui**,[1] **and Huilin Chu**[1]

[1]*School of Safety Engineering, Beijing Institute of Petrochemical Technology, Beijing 102617, China*
[2]*Beijing Academy of Safety Engineering and Technology, Beijing 102617, China*

Correspondence should be addressed to Siyuan Wu; wusiyuan@bipt.edu.cn

Received 3 August 2022; Revised 8 September 2022; Accepted 9 September 2022; Published 24 September 2022

Academic Editor: Ho SoonMin

For the petrochemical industry, the spontaneous burning of iron sulfide compounds has been a major issue. In this study, XRD characterization of samples of iron sulfide compounds with spontaneous combustion tendency revealed that amorphous FeS was the primary constituent of the samples. A molecular simulation was used to build an amorphous FeS cluster model, and the density functional theory was used to examine the adsorption and reactivity characteristics of Fe_4S_4 clusters with O_2. Different adsorption structures are generated by considering different adsorption sites and the electronic characteristics of each adsorption structure are evaluated. The results show that O_2 prefers to adsorb around Fe atoms and has repulsion with S atoms, and the adsorption energy is maximum when two O atoms are co-adsorbed around Fe atoms, which is 198.13 kJ/mol. After adsorption charge, oxygen is in the superoxide state. The calculation of the reaction path divides the reaction process into different stages and considers different reaction routes. A thorough evaluation of the energy barriers and reaction energies of the two exothermic reactions leads to the conclusion that reaction path 1 is the optimal reaction path, and the reaction can release a total of 582.76 kJ/mol of heat. According to calculations, dimeric sulfur S_2 must absorb a large part amount of energy in order to conduct the oxidation process. However, because S_2 is present in the Fe_4S_4 reaction system, it may start the oxidation reaction by absorbing heat from the system and releasing 470.94 kJ/mol of heat. As a result, we conclude that this spontaneous exothermic reaction is a major cause of iron sulfide compounds spontaneous combustion. The thermal oxidation of the dimeric sulfur S_2 generated in the reaction system releases heat that aggregates with the heat from the Fe_4S_4 cluster's oxidation reaction system, eventually causing spontaneous combustion as a result of the heat's continual buildup. In this study, we explore the reason for the extremely easy oxidation and spontaneous burning of iron sulfide compounds from a microscopic perspective to provide a theoretical foundation for the prevention and control of iron sulfide compound spontaneous combustion in the petrochemical sector.

1. Introduction

Due to their distinctive chemical characteristics, transition metal sulfide clusters have drawn considerable interest in a number of disciplines, including materials science, geophysics, catalysis, and biology. There have been efforts to investigate these characteristic features from a microscopic perspective. In recent years, quantum chemical computation techniques based on the density functional theory have given an efficient means of investigating these transition metal complexes. This approach has been widely used in the investigation of transition metal complex adsorption and reaction processes. For example, studies on the interaction of water and the surface of $CuAl_2O_4$ [1], adsorption of Fe, Co, Ni, and other metals on the surface of $CuAl_2O_4$ [2], the electronic structure and magnetic aspects of monolayer MoS_2 doped with 3d transition metal atoms and metal oxide clusters [3], and the mechanism of the acetylene hydrogenation reaction catalyzed by FeO, Fe_2O_3, Fe_3O_4 clusters [4], etc. The approach gives information on substances at the molecular level.

Currently, iron-sulfur clusters are frequently used as models in theoretical investigations of sulfur-iron complexes. These iron-sulfur clusters have alternating iron-sulfur bonding, and planar rhombic [2Fe-2S] assembly

generates bigger size iron-sulfur clusters [5, 6]. Knowing how to correctly describe the magnetic and structural characteristics of iron-sulfur clusters is one of the challenges faced by theoretical workers. Photoelectron spectroscopy (PES) studies of $(FeS)_m$ indicate that these iron-sulfur clusters may have multiple spin states. The iron-sulfur system is usually described by DFT, CASSCF, and CASPT2 methods in theoretical calculations [7–9]. However, the properties calculated by different generalized methods deviate from the experimental values. For example, parameters such as vertical ionization potential (VIP) and adiabatic electron affinity energy (AEA) differ greatly from experimental values. Amitouche et al. [10], Li et al. [11], and Yin et al. [12] tested the structure of the iron-sulfur system using a variety of generalized functions in combination with basis groups. Among them, the B3LYP generalized function and the PBE generalized function agree well with the experimental values, and these two generalized functions are consistent in describing the spin states of the iron-sulfur clusters, but both methods underestimate the experimental values of the interatomic distances in terms of structural properties. For the vibrational frequencies, the calculated results of B3LYP differ from the experimental values by 20%, while the PBE functional only differs from the experimental values by 6%. In addition, the two methods are consistent in the description of the adiabatic electron affinity energy (AEA) and the vertical ionization potential (VDE). Tazibt et al. [13] investigated the structure and magnetic properties of pure Fe clusters, on the basis of which the effect of doping with sulfur elements on the pure Fe cluster system was examined. The results show that the doping of sulfur with Fe enhances the binding energy of the atoms but has no significant effect on the magnetic properties of the system, implying that the magnetic properties of the iron-sulfur clusters are mainly dominated by the Fe atoms.

Because the outermost d orbital of Fe atom in the iron-sulfur cluster contains unpaired single electrons, the iron-sulfur cluster has good reactivity [14, 15]. Iron-sulfur clusters were found to be very sensitive to oxygen (O_2), carbon monoxide (CO), and nitric oxide (NO) in the study. When iron-sulfur clusters are in contact with gases such as O_2, NO, and CO, CO and NO reduce the spin polarization and change the magnetic coupling of the clusters, and the reduction of spin polarization is reflected in the transition metal cluster atoms, especially the Fe atoms in contact with C or N. The effect of O_2 chemisorption on the spin-polarized electronic structure is also quite significant, with oxygen tending to strongly decrease the spin polarization of Fe atoms and weaken Fe-Fe interactions, inducing antiparallel coupling. Heim et al. [16] performed kinetic measurements of the interaction of iron-sulfur clusters with N_2 in an ion trap. The results show that iron-sulfur clusters can adsorb N_2, and in addition, they present the first experimentally obtained binding energy of N_2 with iron-sulfur clusters. Sandra M. Lang et al. [17] proposed that the reaction of iron-sulfur clusters with oxygen follows an oxygen-sulfur exchange mechanism, but this mechanism can only occur in a proton-free environment, while the oxidation reaction performance of iron-sulfur clusters will be better when water is present in the reaction environment [18].

Active sulfur corrosion of equipment surfaces during crude oil refining and storage in the petrochemical sector frequently creates iron sulfide compounds that are prone to spontaneous combustion when exposed to oxygen or air. These iron sulfide compounds exhibit distinct electrical properties as well as exceptionally strong oxidation properties. Mackinawite [19], Cubic FeS [20–22], and pyrite had previously been recognized as the primary iron sulfide compounds. These iron sulfide compounds have amorphous structures [23] and are often loose and porous. For a long time, most investigations on this subject were conducted using experimental approaches, which cannot give insights into the microscopic mechanisms of iron sulfide compounds' oxidation. This study uses the density functional theory to investigate the interactions between oxygen and iron-sulfur clusters, including oxygen adsorption, charge distribution, and reaction pathways. This offers a molecular-level understanding of the process underlying iron sulfide compound spontaneous combustion.

2. Computational Methods and Models

2.1. Computational Methods. In this work, we use the Dmol^3 [24] module in Materials Studio software based on the density functional theory. We use the Perdew–Burke –Ernzerhof (PBE) [25] exchange-correlation generalization in the generalized gradient approximation (GGA) [26]. We choose the double numerical extended basis group (DNP) for all-electron calculations. The accuracy of the structural optimization parameters is fine, the energy convergence is $1.0\,e-5$ Ha, the maximum force convergence is 0.002 Ha/Å, the maximum displacement convergence is 0.005 Å, and the self-consistent field (SCF) accuracy is set to $1.0 * 10^{-6}$ ev. Because the iron sulfide compound system contains transition metal Fe, the 3d orbitals contain unpaired single electrons. Therefore, the ground state configuration of the system is in the high spin state. In previous studies, it was pointed out that the most stable configuration of the ground state of the Fe_4S_4 structure is the nine-fold state. Therefore, the calculations are performed in the nine-fold state in this work. It should be noted that the ground state stable structure of the oxygen molecule is the triplet state. The structures of O_2 molecules and Fe_4S_4 clusters were optimized, respectively, and frequency calculations were performed on all optimized configurations. The vibration frequency results were all positive values, indicating that the optimized structure is a stable configuration on the potential energy surface. We use the LST/QST method to search and optimize the transition state and calculate the frequency of the transition state to ensure that there is a unique virtual frequency in the transition state. The adsorption energy is defined as follows:

$$E_{\text{ads}} = E_{O_2/\text{FeS}} - E_{O_2} - E_{\text{FeS}}, \tag{1}$$

where E_{ads} is the adsorption energy, $E_{O2/\text{FeS}}$ is the total energy of the model after adsorption, E_{O2} is the total energy of the oxygen molecule, and E_{FeS} is the total energy of the iron sulfide cluster. According to the definition, the negative

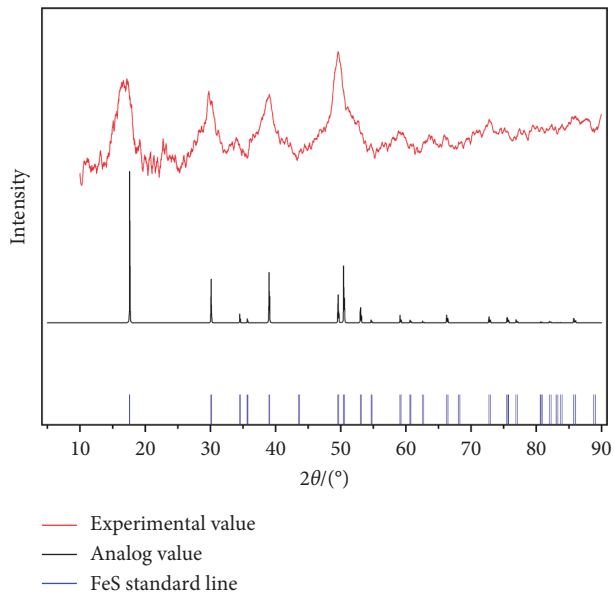

Figure 1: Comparison of the experimental X-ray diffraction pattern of active iron sulfide compounds sample with simulated X-ray diffraction pattern of FeS crystal model.

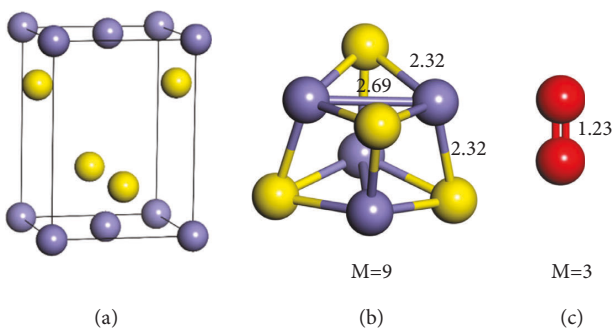

Figure 2: (a) FeS crystal model. (b) Fe_4S_4 cluster model. (c) O_2 structure model. (Purple represents Fe atoms, yellow represents *S* atoms, and red represents O atoms). *M* represents spin multiplicity; bond length unit: Å.

value of the adsorption energy indicates the exothermic process, and the larger the value, the stronger the adsorption of O_2 and Fe_4S_4 clusters.

2.2. Computational Models. In this work, XRD characterization of iron sulfide samples with spontaneous combustion tendency was carried out and is shown in red in Figure 1. It can be seen from the diffraction peaks in the figure that the crystallinity of the sample is poor, and the type of peak is a typical amorphous structure diffraction peak. Compared with the standard FeS diffraction pattern, the sample is amorphous FeS.

The FeS crystal structure was found in the inorganic crystal database, as illustrated in Figure 2(a). The FeS crystal structure's XRD diffraction pattern was acquired by scanning the FeS crystal structure using the Reflex software, as demonstrated by the diffraction peaks highlighted in black in Figure 1.

Comparisons were made between the experimental and simulated X-ray diffraction patterns. The X-ray diffraction peaks in the experiment appear at 16.7°, 30°, 38.8°, and 49.9°. The simulated X-ray diffraction peaks appear at corresponding angles of 17.6, 30.1, 39, and 50.45°. In other words, the discrepancy between the simulated and experimental diffraction peaks is kept to a maximum of 1°. Based on the FeS crystal model, the Fe_4S_4 cluster model was created. The cluster structure was then optimized and the result is shown in Figure 2(b). The optimized cluster structure was compared with previous research data [10] to confirm the reasonableness of the calculation method and structure used in this work, and the results of the comparison are provided in the supporting information. *M* denotes the spin multiplet degree. The bond length of the triplet state of the ground state oxygen molecule is 1.23 Å (as shown in Figure 2(c)).

3. Results and Discussion

3.1. Adsorption of O_2 on Fe_4S_4 Clusters. On Fe and S sites, respectively, we took into account O_2 adsorbed. Each adsorption location is subdivided into three adsorption modes: O_2 adsorbed at one end, O_2 adsorbed at both ends, and O_2 adsorbed at the Fe-S bond bridge location. To obtain stable adsorption structures, structural optimization and frequency calculations were done for each adsorption model (as shown in Figures 3 and 4). The information in Figure 5 includes the adsorption schematic and the adsorption energy for each adsorption struture.

From Figure 3(a), it can be seen that when two oxygen atoms are co-adsorbed on Fe atoms, the two Fe-O bonds formed have lengths of 2.08 Å and 2.09 Å, respectively, and the O-O bond grows from 1.23 Å to 1.34 Å in the ground state. It can be seen from the charge density diagram that a large number of charges are distributed around the Fe-O bond after O_2 adsorption, which indicates that O_2 forms chemisorption with Fe_4S_4. From the Mulliken charge population analysis (Table 1), a total of 0.35 e electrons were obtained by O_2 after adsorption and the adsorption energy of this adsorption mode is −198.13 kJ/mol. In Figure 3(b), O_2 was adsorbed on Fe atoms with one end and the O-O bond grew from the ground state of 1.23 Å to 1.30 Å The charge density diagram showed that a large number of charges were distributed around the Fe-O bond, indicating that this adsorption mode also belongs to chemisorption. It is calculated that O_2 adsorption gains a total of 0.28 e electrons and the adsorption energy is −43.11 kJ/mol. In Figure 3(c), when O_2 is adsorbed at the bridge site, the O-O bond length differs very little from the ground state bond length, and the distances between the two oxygen atoms and the Fe and S atoms are 3.67 Å and 3. 73 Å, respectively. It can be seen from the charge density diagram that there is no charge distribution between the O_2 and Fe_4S_4 clusters and the Mulliken charges of the two O atoms are −0.06 and −0.08, respectively, indicating that this O2 did not involve in chemisorption with the Fe4S4 cluster. The calculated adsorption energy is 10.94 kJ/mol and this adsorption mode does not form a stable adsorption structure.

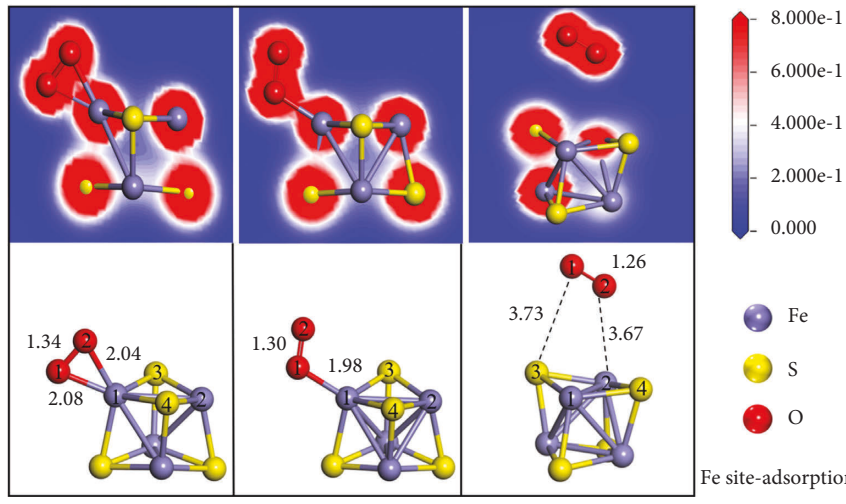

Figure 3: Adsorption structures of O_2 on Fe sites on Fe_4S_4 clusters and the charge density of each adsorption structure. The bond lengths in the figure are in Å, 1 Å = 1 ∗ 10^{-10} m; the blue part of the charge density diagram indicates no charge aggregation, and the red part indicates charge aggregation.

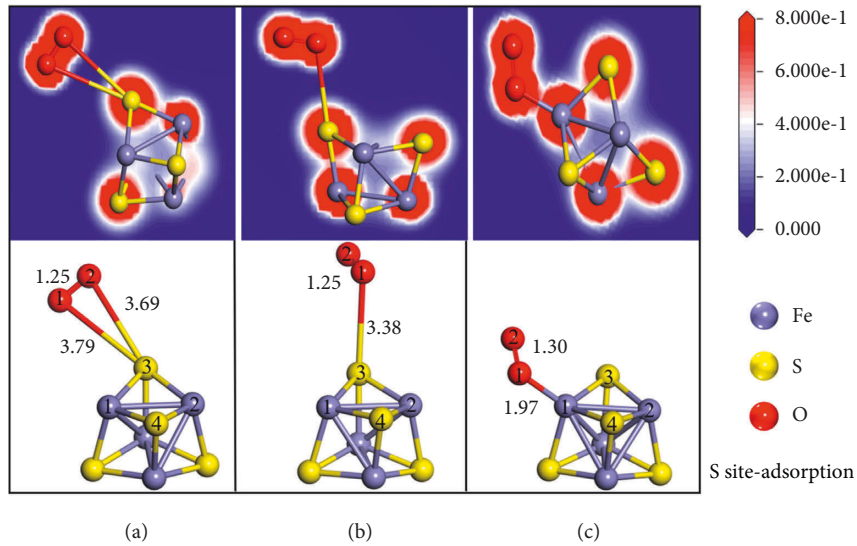

Figure 4: Adsorption structures of O_2 on *S* sites on Fe_4S_4 clusters and the charge density of each adsorption structure. The bond lengths in the figure are in Å, 1 Å = 1 ∗ 10^{-10} m; the blue part of the charge density diagram indicates no charge aggregation, and the red part indicates charge aggregation.

Table 1: Mulliken atomic population values of O atoms before and after adsorption.

Figure	*Before adsorption*		*After adsorption*	
	O1	O2	O1	O2
A	0	0	−0.18	−0.17
B	0	0	−0.17	−0.11
C	0	0	−0.06	−0.08
d	0	0	−0.05	−0.06
e	0	0	−0.06	−0.05
f	0	0	−0.17	−0.10

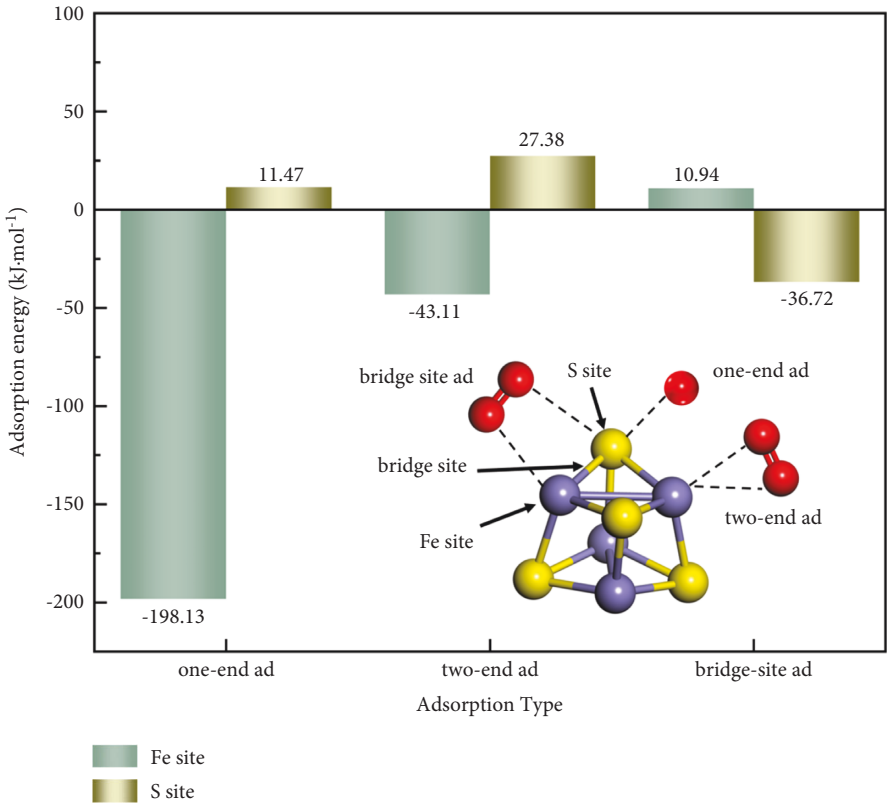

Figure 5: Adsorption energy of O_2 on Fe_4S_4 clusters. (ad represents adsorption).

When O_2 is adsorbed at the S position, as shown in Figures 4(d)–4(f), O_2 shows strong repulsion with Fe_4S_4 in one-end adsorption and two-end adsorption. The charge density diagram shows that there is no charge distribution between O_2 and Fe_4S_4 clusters, and the O-O bond length is not much different from the ground state bond length. Mulliken's atomic population also show no large charge transfer after O_2 adsorption. This indicates that O_2 will not adsorb at the *S* site. The adsorption energies of these two adsorption structures are 11.47 kJ/mol and 27.38 kJ/mol, respectively. The adsorption energy is positive, indicating that no chemical adsorption will be formed. In Figure 4(f), we examine O_2 adsorption at the Fe-S bridge site; however, the calculations show that there is a repulsion between the O atom and the S atom and the other O atom forms a Fe-O bond with the Fe atom; this adsorption is similar to the O_2 adsorption structure at one end of the Fe site with an O-O bond length of 1.30 Å and adsorption energy of −36.72 kJ/mol.

The abovementioned analysis shows that O_2, when adsorbed in the molecular state, tends to adsorb around Fe atoms on the Fe_4S_4 cluster and not around S atoms. The energy of 198.13 kJ/mol is released when two O atoms are co-adsorbed on Fe atoms, which provides the energy basis for the subsequent reaction process.

3.2. Reaction Path Calculation. The reaction path of Fe_4S_4 with O_2 was computed in this study, with the first two reaction stages occurring on the nine-fold state potential energy surface, and the last reaction stage occurring on the three-fold state potential energy surface. The initial stage of the reaction is the formation of the stage products $Fe_2S_2O_2$ and dimeric sulfur (S_2) from Fe_4S_4 and O_2. As the reaction proceeds, new O atoms continue to react with these products to form FeO and dimeric sulfur (S_2). It should be noted that dimeric sulfur (S_2) is formed at different stages of the reaction and is eventually oxidized to SO_2. The reaction potential energy profiles are given in Figures 6–8, where the initial adsorption structure is denoted by *R*, TS represents the transition state, and IM represents the intermediate. The initial reactant energy is used as the zero point to compute the energy difference of each intermediate, transition state, and product with regard to the reactants. Table 2 shows the unique imaginary frequencies of the reaction path's transition states.

3.3. Reaction Path Analysis

3.3.1. Stage 1: Fe_4S_4 Reacts with O_2 to Form $Fe_4S_2O_2$ and S_2. When the Fe_4S_4 cluster comes in contact with O_2, O_2 preferentially adsorbs on the Fe atom of the Fe_4S_4 cluster to form the composite reactant *R*1. As shown in Figure 6, the reactions are discussed in two pathways depending on the different intermediates. The formation of the complex reactant *R* is an exothermic reaction. It was calculated that the process released 198.13 kJ/mol of energy. The reactant *R* forms the stable intermediate IM1 through the transition state TS1, during which the O-O bond breaks and the O

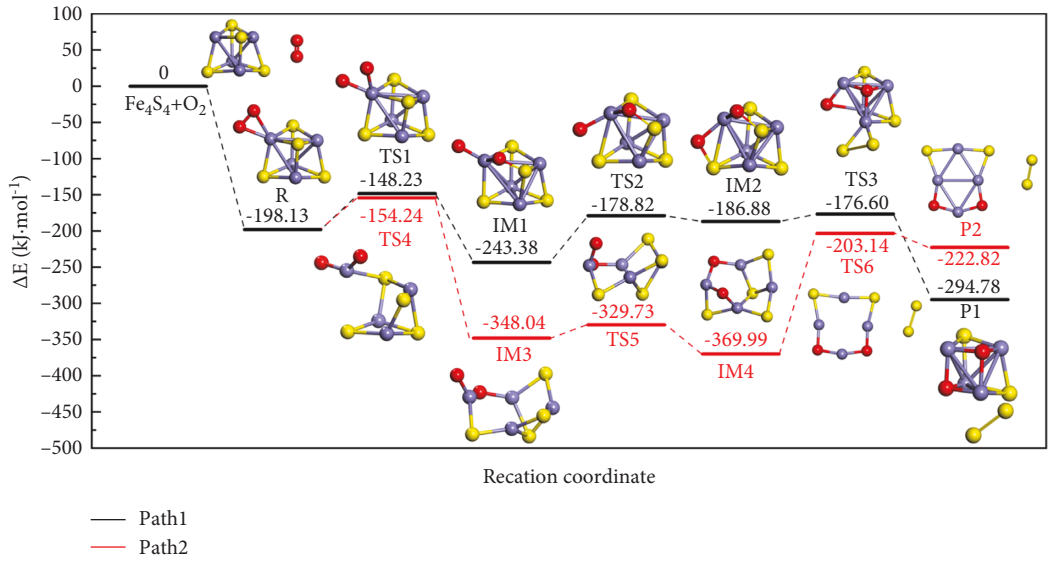

Figure 6: The stage 1 reaction path of Fe_4S_4 clusters with O_2 on the nine-fold state potential energy surface.

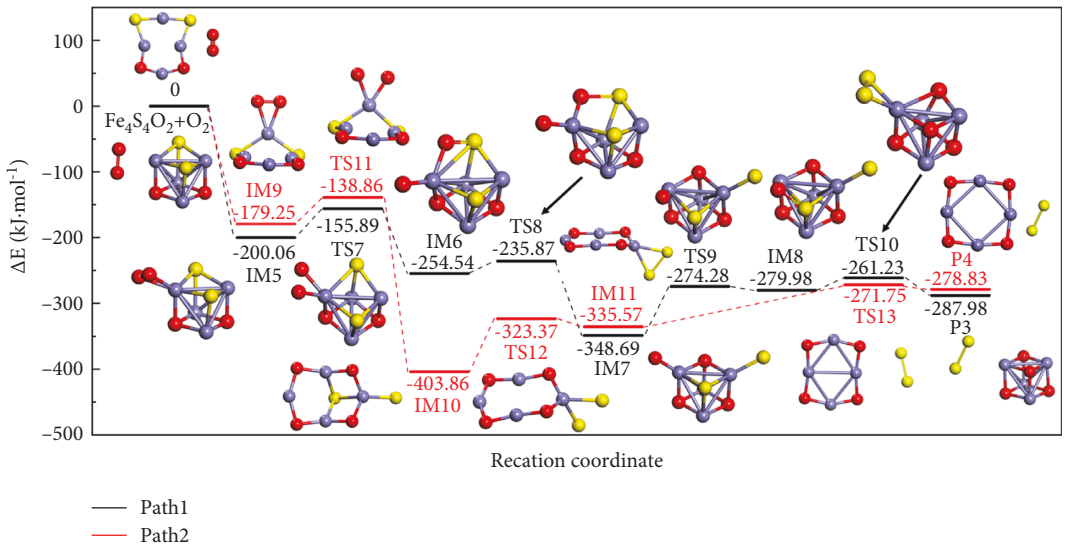

Figure 7: The stage 2 reaction path of Fe_4S_4 clusters with O_2 on the nine-fold state potential energy surface.

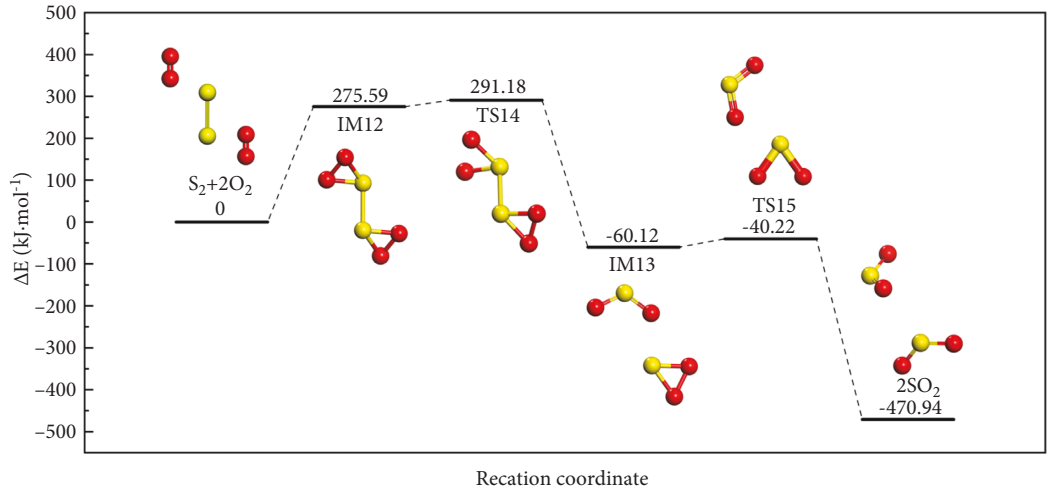

Figure 8: The stage 3 reaction path of S_2 with O_2 on the triplet state potential energy surface.

Table 2: Imaginary frequency of transition state in the reaction between O_2 and Fe_4S_4 clusters.

Species	Frequency/cm^{-1}
TS1	−483.77
TS2	−241.04
TS3	−62.04
TS4	−46.10
TS5	−91.56
TS6	−14.76
TS7	−56.66
TS8	−41.79
TS9	−264.29
TS10	−119.14
TS11	−404.57
TS12	−126.30
TS13	−9.41
TS14	−638.53
TS15	−744.97
—	—

atom attacks the flanking S atom to form an S-O bond, a process that requires overcoming an energy barrier of 49.9 kJ/mol. Intermediate IM1 overcomes the energy barrier of 64.56 kJ/mol to form intermediate IM2, and another O atom in O_2 attacks the S atom below to form an S-O bond. The energy barrier of 10.28 kJ/mol formed by the transition state TS3 needs to be overcome from the intermediate IM2 to the formation stage product P1. Two S atoms in this process form dimeric sulfur S_2, and the remaining part is the incompletely reacted $Fe_4S_2O_2$.

In reaction path 2, reactant *R* passes through the transition state TS4 to form intermediate IM3, a process that requires an energy barrier of 43.89 kJ/mol to be overcome. This process breaks the O-O bond, one of the O atoms is bonded to a Fe atom on one side. Intermediate IM3 passes through the transition state TS5 to form intermediate IM4, which requires an energy barrier of 18.31 kJ/mol to be overcome. This process involves the formation of a Fe-O bond by another O atom with the Fe atom below. Thereafter, two S atoms in intermediate IM4 form S_2, a step that requires a large energy barrier to be experienced to proceed, which is calculated to be 166.85 kJ/mol for the formation of transition state TS6.

In stage 1, the two reaction routes proceed through distinct intermediates and transition states to yield products P1 and P2. Both P1 and P2 are $Fe_4S_2O_2$ and dimeric sulfur S_2. The difference is that $Fe_4S_2O_2$ in P1 is a blocky structure, while $Fe_4S_2O_2$ in P2 is a planar structure. From the stage 1 reaction as a whole, the reaction of Fe_4S_4 with O_2 to form $Fe_4S_2O_2$ and S_2 is similar to the substitution of sulfur atoms in Fe_4S_4 by oxygen atoms, which is consistent with the iron-sulfur cluster oxidation mechanism proposed by Sandra M. Lang et al. [17]. $Fe_4S_2O_2$ and S_2 will continue to react upon exposure to new O_2, which we discuss in the reaction of stage 2.

3.3.2. Stage 2: $Fe_4S_2O_2$ Reacts with O_2 to Form 4FeO and S_2. When the reaction product $Fe_4S_2O_2$ in stage 1 continues to react with O_2, O_2 also preferentially adsorbs around the Fe atom. This stage of the reaction takes into account the different intermediates and transition states, and we divide it into two reaction paths for discussion. Path 1 and path 2 correspond to the two paths in stage 1. O_2 adsorption on the $Fe_4S_2O_2$ cluster releases 200.06 kJ/mol of energy to form intermediate IM5, and after the transition state TS7 to form intermediate IM6, the O-O bond breaks in this step and one of the O atoms attacks the S atom to form an S-O bond, a process that requires overcoming an energy barrier of 44.17 kJ/mol. Intermediate IM6 overcomes the energy barrier of 18.67 kJ/mol passing through the transition state TS8 to form intermediate IM7. The S atom is replaced out of its original ligand environment during this process. Subsequently, another O atom attacks the S atom to form an S-O bond, as shown in IM8 in Figure 7. This step requires overcoming an energy barrier of 74.41 kJ/mol. IM8 passes through the transition state TS10 to form product P3. This process overcomes the energy barrier of 18.75 kJ/mol and the S atom is completely replaced out of the original ligand environment to form dimeric sulfur S_2 and FeO.

In path 2, O_2 adsorbed on Fe atoms releases 179.25 kJ/mol of energy to form intermediate IM9. IM9 overcomes the energy barrier of 40.39 kJ/mol and passes through the transition state TS11 to form intermediate IM10. After the O-O bond is broken, the O atom attacks the S atom to break the Fe-S bond. Subsequently, the O atom will continue to attack the sulfur atom leading to the complete reaction of the S atom and the formation of intermediate IM11. This process can proceed by overcoming an energy barrier of 80.5 kJ/mol. The intermediate IM11 overcomes an energy barrier of 63.83 kJ/mol to form the product P4. The two products of this stage, P3 and P4, are both FeO and dimeric sulfur (S_2).

When seen as a whole, the stage reaction is effectively a continuous reaction process, with stage 2 occurring after stage 1. FeO and S_2 are eventually produced in both phases of the reaction. Because FeO is unstable, it will progressively oxidize in the environment to generate Fe_2O_3, a process that is thought to occur naturally and is not further explored in this research.

3.3.3. Stage 3: S_2 Reacts with $2O_2$ to Form $2SO_2$. Because SO_2 is released during the oxidation of Fe_4S_4, the subsequent reaction of dimeric sulfur S_2 is further investigated in this paper. The oxidation of S_2 is treated as the third stage of the reaction in this work, but it does not occur exactly after the first two stages in time because S_2 is generated in both of the first two processes. The oxidation of S_2 takes place on the triplet potential energy surface. S_2 interacts with O_2 to form SO_2, and the initial step of the reaction requires 275.59 kJ/mol energy absorption. As a result, under ambient circumstances, S_2 does not oxidize. However, the initial two stages of the oxidation reaction system of iron sulfide compounds emit a significant amount of heat, raising the temperature of the entire reaction system and providing a reaction foundation for the oxidation of S_2. When S_2 has absorbed sufficient heat, the reaction can proceed by only overcoming a small energy barrier. At this stage, the S-S bond breaks and the S atom attacks O_2 to form the SO_2 molecule. To form SO_2, the intermediate IM13 merely has to overcome a potential barrier of 19.9 kJ/mol.

Table 3: Heat of reaction for each phase of the reaction.

Process		Reaction path	Heat of reaction/kJ·mol^{-1}
Stage1	Path1	$Fe_4S_4+O_2 \longrightarrow P1$	−294.78
	Path2	$Fe_4S_4+O_2 \longrightarrow P2$	−222.82
Stage2	Path1	$Fe_4S_2O_2 \longrightarrow P3$	−287.98
	Path2	$Fe_4S_2O_2 \longrightarrow P4$	−278.83
Stage3		$S_2+2O_2 \longrightarrow 2SO_2$	−470.94

The reaction between Fe_4S_4 and O_2 is exothermic at every stage, which is advantageous thermodynamically. The heat of reaction for each stage is displayed in Table 3. On adsorption in the first stage of the reaction, the two reactants in path 1 generated 198.13 kJ/mol of heat, which laid the groundwork for the subsequent reaction. The reaction between reactant *R* and stage product P1 is exothermic. The maximal energy barrier encountered throughout this process is 64.56 kJ/mol, and the heat emitted at the start of the reaction is enough to keep the reaction going. The heat released from reaction path 1 is calculated to be 294.78 kJ/mol. In contrast, the maximum energy barrier to be overcome in reaction path 2 is 166.85 kJ/mol required to pass through TS6, and the release of 369.99 kJ/mol from the start of the reaction to the formation of intermediate IM5 is sufficient to support the reaction. Therefore, reaction path 1 is more likely to occur than reaction path 2 in comparison.

Overall, the stage's two chemical paths are both exothermic, with path 1 releasing 287.98 kJ/mol of heat and path 2 releasing 278.83 kJ/mol of heat. The largest energy barrier to cross in reaction path 1 is 74.41 kJ/mol. The largest energy barrier that must be overcome in reaction path 2 is 80.49 kJ/mol. Reaction path 1 facilitates the reaction's progression more than reaction path 2. In the oxidation of Fe_4S_4 clusters, reaction path 1 is the optimum reaction channel. However, whether reaction path 1 or reaction path 2, the reaction products are FeO and S_2, and the entire reaction process is exothermic.

There may be no SO_2 release at the start of the reaction because the S_2 yield and heat released by the reaction system are insufficient to sustain the oxidation of dimeric sulfur S_2. Dimer sulfur S_2 is gradually oxidized as the reaction progresses, and as the reaction system continues to build up heat, it will encourage the oxidation of dimer sulfur S_2 and release a significant quantity of heat, which raises the reaction system's temperature once more. Table 3 shows that the heat of the S_2 oxidation reaction in stage 3 is 470.94 kJ/mol. Therefore, the oxidative exothermic process of S_2 has a nonnegligible effect on the spontaneous combustion of iron sulfide compounds.

4. Conclusion

In this work, XRD analysis of iron sulfide compound samples with spontaneous combustion activity was done, structural models of Fe_4S_4 and O_2 were built using molecular simulations, and interactions between Fe_4S_4 clusters and O_2 were computed at the GGA/PBE level, leading to the following primary results:

The iron sulfide compound sample's XRD pattern revealed that it did not have any obvious crystalline diffraction peaks, indicating that it had an amorphous structure. Analysis of the peaks' peak locations also revealed that the sample was an amorphous FeS.

Calculations of the adsorption parameters of O_2 and Fe_4S_4 clusters demonstrate that when adsorbed with Fe_4S_4, O_2 tends to adsorb around Fe atoms and the adsorption energy of O_2 is greatest when adsorbed at both ends. When O_2 is adsorbed at the Fe-S bridge site, there is no charge transfer between the two and no stable chemisorption is created. It was discovered that there was a repulsion between O and S atoms in the computation of O_2 adsorption at S sites, and there was no charge transfer between O_2 and Fe_4S_4 clusters for either end adsorption or both ends adsorption. When O_2 is adsorbed at the Fe-S bridge site, the optimized O_2 is stabilized around the Fe atom and one of the O atoms is attached to the Fe atom, similar to how O_2 is adsorbed at one end of the Fe site. In conclusion, O_2 does not stably adsorb close to S atoms.

The reaction path analysis of Fe_4S_4 with O_2 is examined by splitting the reaction into 3 stages, the first two of which are effectively the same reaction process. We analyzed the reaction energy barrier and reaction energy for reaction paths 1 and 2 in both stages of the reaction. Reaction path 1 is the ideal reaction path, according to the analysis. The total exergy of reaction path 1 is calculated to be 582.76 kJ/mol. The total energy of reaction path 2 is 501.65 kJ/mol. In this study, the oxidation of dimeric sulfur produced in the first two reaction stages was also analyzed. It was discovered that while the oxidation reaction of dimeric sulfur S_2 requires some energy to be absorbed to proceed, a lot of energy is released once the reaction is started. The oxidation reaction of S_2 is calculated to release 470.94 kJ/mol of energy.

Therefore, we believe that the oxidation reaction of Fe_4S_4 is a multistage exothermic reaction that can proceed spontaneously, with S_2 being continuously generated during the reaction, and the generated S_2 absorbs energy in the oxidation reaction system of Fe_4S_4 to undergo oxidation reactions and release large amounts of heat, accompanied by the release of SO_2. This speeds up the oxidation of Fe_4S_4, which increases the temperature of the reaction system until spontaneous combustion happens.

Data Availability

The original data used to support the findings of this work can be obtained from the corresponding author upon request.

Conflicts of Interest

The authors declare that there are no conflicts of interest.

Acknowledgments

This work was supported by Beijing Natural Science Foundation (No. 2214071); National-level Undergraduate Innovation and Entrepreneurship Program (URT) Project

(2022J00089); and the Beijing University Student Innovation and Entrepreneurship Program (Urt) Project (2021J00110).

Supplementary Materials

Supplementary materials contain accuracy tests of computational methods and information on the structure of the ground state. (*Supplementary Materials*)

References

[1] L. Shi, S. Meng, S. Jungsuttiwong et al., "High coverage H_2O adsorption on $CuAl_2O_4$ surface: a DFT study," *Applied Surface Science*, vol. 507, no. 30, 2020.

[2] L. Li, Y. M. Gan, Z. H. Lu et al., "The effects of Fe, Co and Ni doping in $CuAl_2O_4$ spinel surface and bulk: a DFT study," *Applied Surface Science*, vol. 521, no. 15, Article ID 146478, 2020.

[3] D. Li, Y. Niu, H. Zhao, C. Liang, and Z. He, "Electronic and magnetic properties of 3d-metal trioxides superhalogen cluster-doped monolayer MoS2: a first-principles study," *Physics Letters A*, vol. 378, no. 22-23, pp. 1651–1656, 2014.

[4] R. Feng, L. Pan, F. Li et al., "The kinetic mechanism of acetylene hydrogenation to prepare ethane over FexOy clusters: a DFT study," *Chemical Engineering Science*, vol. 230, Article ID 116170, 2021.

[5] S. M. Lang, K. Miyajima, T. M. Bernhardt, F. Mafune, R. N. Barnett, and U. Landman, "Thermal stability of iron-sulfur clusters," *Physical Chemistry Chemical Physics*, vol. 20, no. 11, pp. 7781–7790, 2018.

[6] S. Yin and E. R. Bernstein, "Photoelectron spectroscopy and density functional theory studies of iron sulfur $(FeS)_m^-$ ($m = 2$–8) cluster Anions: coexisting multiple spin states," *The Journal of Physical Chemistry A*, vol. 121, no. 39, pp. 7362–7373, 2017.

[7] Z. J. Wu, M. Y. Wang, and Z. M. Su, "Electronic structures and chemical bonding in diatomic ScX to ZnX (X = S, Se, Te)," *Journal of Computational Chemistry*, vol. 28, no. 3, pp. 703–714, 2007.

[8] B. Liang, X. Wang, and L. Andrews, "Infrared spectra and density functional theory calculations of group 10 transition metal sulfide molecules and complexes," *The Journal of Physical Chemistry A*, vol. 113, no. 14, pp. 3336–3343, 2009.

[9] S. Clima and M. F. A. Hendrickx, "Interpretation of the photoelectron spectra of FeS2- by a multiconfiguration computational approach," *The Journal of Physical Chemistry A*, vol. 111, no. 43, pp. 10988–10992, 2007.

[10] F. Amitouche, F. Saad, S. Tazibt, S. Bouarab, and A. Vega, "Structural and electronic rearrangements in Fe2S2, Fe3S4, and Fe4S4 atomic clusters under the attack of NO, CO, and O2," *The Journal of Physical Chemistry A*, vol. 123, no. 51, pp. 10919–10929, 2019.

[11] Y. N. Li, S. Wang, T. Wang et al., "Energies and spin states of FeS0/−, FeS20/−, Fe2S20/−, Fe3S40/−, and Fe4S40/− clusters," *ChemPhysChem*, vol. 14, no. 6, pp. 1182–1189, 2013.

[12] S. Yin, Z. Wang, and E. R. Bernstein, "Formaldehyde and methanol formation from reaction of carbon monoxide and hydrogen on neutral Fe2S2 clusters in the gas phase," *Physical Chemistry Chemical Physics*, vol. 15, no. 13, pp. 4699–4706, 2013.

[13] S. Tazibt, A. Chikhaoui, S. Bouarab, and A. Vega, "Structural, electronic, and magnetic properties of iron disulfide $Fe_nS_2^{0/\pm}$ ($n = 1$–6) clusters," *The Journal of Physical Chemistry A*, vol. 121, no. 19, pp. 3768–3780, 2017.

[14] S. Tazibt, S. Bouarab, A. Ziane, J. C. Parlebas, and C. Demangeat, "Electronic, magnetic and structural properties of neutral, cationic and anionic Fe2S2, Fe3S4 and Fe4S4 clusters," *Journal of Physics B: Atomic, Molecular and Optical Physics*, vol. 43, no. 16, 2010.

[15] L. P. Ding, X. Y. Kuang, P. Shao, and M. M. Zhong, "Probing the structural, electronic and magnetic properties of multi-center Fe2S2 0/-Fe3S4 0/- and Fe4S4 0/- clusters," *Journal of Molecular Modeling*, vol. 19, no. 4, pp. 1527–1536, 2013.

[16] H. C. Heim, T. M. Bernhardt, S. M. Lang, R. N. Barnett, and U. Landman, "Interaction of iron—sulfur clusters with N2: biomimetic systems in the gas phase," *Journal of Physical Chemistry C*, vol. 120, no. 23, pp. 12549–12558, 2016.

[17] S. M. Lang, R. N. Barnett, and U. Landman, "Oxygen sensitivity of free nonligated iron—sulfur clusters," *Journal of Physical Chemistry C*, vol. 123, no. 45, pp. 27681–27689, 2019.

[18] N. Y. Dzade, A. Roldan, and N. H. de Leeuw, "DFT-D2 study of the adsorption and dissociation of water on clean and oxygen-covered {001} and {011} surfaces of mackinawite (FeS)," *Journal of Physical Chemistry C*, vol. 120, no. 38, pp. 21441–21450, 2016.

[19] P. Bai, S. Zheng, H. Zhao, Y. Ding, J. Wu, and C. Chen, "Investigations of the diverse corrosion products on steel in a hydrogen sulfide environment," *Corrosion Science*, vol. 87, pp. 397–406, 2014.

[20] D. Rickard and G. W. I. Luther, "Chemistry of iron sulfides," *ChemInform*, vol. 38, no. 19, pp. 514–562, 2007.

[21] S. Nesic, "Key issues related to modelling of internal corrosion of oil and gas pipelines—a review," *Corrosion Science*, vol. 49, no. 12, pp. 4308–4338, 2007.

[22] J. Ning, Y. Zheng, D. Young, B. Brown, and S. Nesic, "Thermodynamic study of hydrogen sulfide corrosion of mild steel," *Corrosion Science*, vol. 70, no. 4, pp. 375–389, 2014.

[23] D. Rickard and G. W. Luther, "Chemistry of iron sulfides," *Chemical Reviews*, vol. 107, no. 2, pp. 514–562, 2007.

[24] B. Delley, "An all-electron numerical method for solving the local density functional for polyatomic molecules," *The Journal of Chemical Physics*, vol. 92, no. 1, pp. 508–517, 1990.

[25] J. P. Perdew and Y. Wang, "Accurate and simple analytic representation of the electron-gas correlation energy," *Physical Review B*, vol. 45, no. 23, pp. 13244–13249, 1992.

[26] J. P. Perdew, K. Burke, and M. Ernzerhof, "Generalized gradient approximation made simple," *Physical Review Letters*, vol. 77, no. 18, pp. 3865–3868, 1996.